Neoclassical Tearing Physics in the Spherical Tokamak MAST

R. J. Buttery, O. Sauter,* R. Akers, M. Gryaznevich, R. Martin, C. D. Warrick, H. R. Wilson, and the MAST Team
EURATOM/UKAEA Fusion Association, Culham Science Centre, Abingdon, Oxfordshire, OX14 3DB, United Kingdom
(Received 6 September 2001; published 11 March 2002)

Results from MAST provide a first test of neoclassical tearing mode physics in the spherical tokamak (ST). The mode accounts for the main performance limit in conventional tokamaks. Its behavior in the ST is remarkably well described by existing theoretical models, although it is more readily seeded by sawtooth events in these scenarios. Modeling confirms the significance of stabilizing field-curvature effects. This provides good grounds for optimism that with suitable control of profiles, it may be possible to avoid these modes in the ST.

DOI: 10.1103/PhysRevLett.88.125005 PACS numbers: 52.55.Tn, 52.35.Py, 52.55.Fa

The study of the neoclassical tearing mode (NTM) in the spherical tokamak (ST) is important, both to test NTM theory, and to assess the potential of the ST as a route to fusion power. A key benefit proposed for the ST is access to high plasma pressures at relatively low toroidal magnetic field (high β—the ratio thermal to magnetic energy), based on arguments relating to ideal magnetohydrodynamic (MHD) stability [1,2]. It was borne out by the START device where β's up to 40% were obtained [3]. However, conventional tokamaks are often limited by NTMs [4,5], which occur below the ideal MHD β limit in hot, low collisionality plasmas. These require a "seeding" instability to be triggered, but degrade confinement, and can lead to disruptions. The new generation of STs such as MAST (up to 2 MA plasma current, 5 MW neutral beam heating, 0.85 m major radius, 0.65 m minor radius) explore power-plant-relevant low collisionality scenarios for the first time. Thus by careful choice of plasma regime on MAST, it has been possible to trigger NTMs, providing the first studies of their behavior in this new scenario.

The definition of an NTM is a magnetic island sustained by the perturbed bootstrap current, that would otherwise ("classically") be tearing stable. The behavior of such an island (of full width "w") can be described by the modified Rutherford equation [6], adopting an approach that is valid at all aspect ratio, based on that in Ref. [7]:

$$\frac{\tau_r}{r^2}\frac{dw}{dt} = \Delta' + \frac{\beta_p}{w}\left(\frac{a_{\rm bs} - a_{\rm GGJ}}{1 + w_d^2/w^2} - \frac{a_{\rm pol}}{w^2}\right), \quad (1)$$

where r is the minor radius of the NTM resonant surface, and τ_r is the resistive time scale. This is expressed in terms of the tearing mode stability parameter (Δ'—negative for NTMs), the perturbed bootstrap current ($a_{\rm bs}\beta_p/w$ term), and the stabilizing effects of field curvature ($a_{\rm GGJ}$) [8], ion polarization currents ($a_{\rm pol}$) [9], and finite island transport (w_d) [10]. The equation leads to a minimum "critical" β_p (the ratio of thermal energy normalized to poloidal magnetic field energy), below which no NTMs can grow. The terms have strongly varying aspect ratio and shape dependencies. For example, it has been predicted that the field curvature term, which represents the stabilizing effect of "good" average magnetic field curvature, will have a large effect at low aspect ratio, and could stabilize the NTM completely in an ST [11]. It is dependent on the resistive interchange parameter, D_R, which scales as $\beta \sim \varepsilon^2\beta_p/q^2$, thus introducing an $\varepsilon^{3/2}$ (ε is inverse aspect ratio) dependence relative to the bootstrap drive (which scales as $\varepsilon^{1/2}\beta_p$). Its exact form must be modified [12] at small w, which further enhances its stabilizing effect. The $a_{\rm pol}$ and w_d terms of Eq. (1) are stabilizing at small island sizes, leading to the requirement of a seeding instability (such as a sawtooth) to trigger the NTM. There remain uncertainties in this physics: the sign of the $a_{\rm pol}$ term is dependent on the island propagation frequency [13], while the w_d term is dependent on the choice of transport model. Thus it is usually left to experimental data to determine the relative roles of these terms.

On MAST we are able to trigger NTMs by operating in a regime with large sawteeth and high β_p. The plasmas used have low collisionality, with typical values of the parameter $\nu = \nu_i/\varepsilon\omega_{e^*} \sim 0.05$ (in terms of ion collision frequency, ν_i, and electron diamagnetic rotation frequency ω_{e^*}), as opposed to the much higher values on START, $\nu \sim 1$ at high β. In these scenarios $3/2$ and $2/1$ modes are frequently observed (denoting as m/n—poloidal/toroidal mode numbers) which appear to degrade the confinement. So far, no higher order modes (such as $4/3$) have been observed on MAST, although common on conventional tokamaks.

A typical discharge is shown in Fig. 1 where as β_p rises (measured by magnetic reconstruction with the EFIT code [14]), successive sawteeth excite first a $3/2$, then a $2/1$ mode (the latter coincident with a transition to high confinement regime—"H mode"). The $3/2$ mode seems fairly benign. The $2/1$ mode initially seems somewhat marginal to growth, with fairly constant amplitude (overlaid on the $n = 1$ spectrogram). However, as β_p rises slightly, at 250 ms the mode starts to grow, and a fall in β_p is subsequently observed. At 281 ms the plasma makes a transition back to L-mode (low) confinement, simultaneous with the mode temporarily locking. The mode rotation then varies as the plasma dithers between L- and H mode, finally locking again at 320 ms, with, a disruption 13 ms later as the plasma current is ramped down. A cylindrical

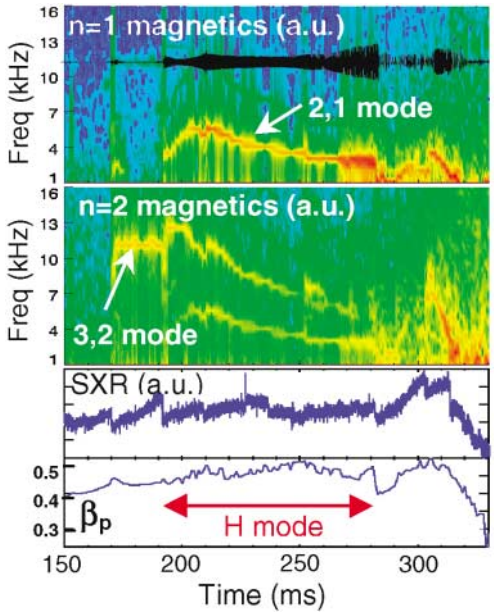

FIG. 1 (color). Spectrograms of $n = 1$ (with amplitude overlaid) and $n = 2$ magnetics, line integrated core soft x ray emission, and β_p for a typical NTM discharge, shot 2952.

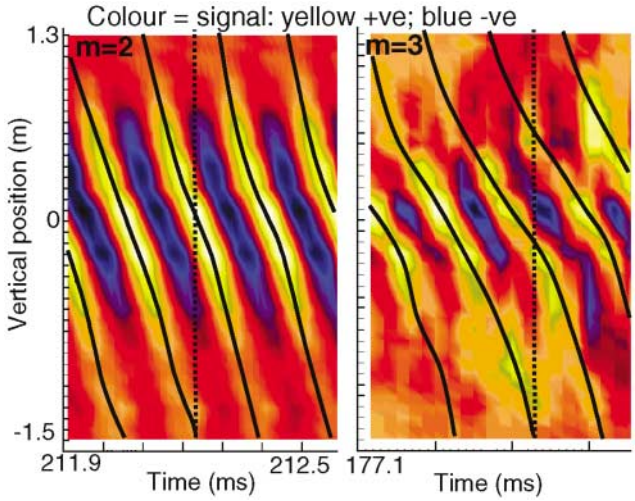

FIG. 2 (color). $m = 2$ and $m = 3$ modes identified by magnetic detectors up the center column of the machine for shot 2952; color indicates magnetic field amplitude with yellow positive, blue negative.

approximation gives the $3/2$ island width $\sim$3 cm, and the peak $2/1$ island width $\sim$10 cm (18% of minor radius)—a scale likely to affect performance. These estimates are confirmed (within 25%) by 3D field line tracing calculations in realistic geometry. Here the plasma representation is matched to EFIT reconstructions, and the island is approximated by a sheet current perturbation inserted at the rational surface with toroidally sinusoidal current variation matching the observed amplitude at the detector.

The toroidal mode numbers have been clearly identified by a toroidal array of magnetic detection coils on the center column. The identification of the poloidal mode numbers is shown in Fig. 2, where magnetic signals up the center column are shown, which pick up most of the mode structure in these tight aspect ratio plasmas (the islands have less than half the vertical extent of the coil array). The $m = 2$ mode is very clear, undergoing 1.7 oscillations down the center column's length. The $m = 3$ mode undergoes $\sim$2.5 oscillations down the center column—this is harder to clearly distinguish, as signals from this more central mode fall off rapidly with distance (as $1/r^{m+1}$). Note also the local pitch on the midplane is steeper than for the $m = 2$ mode, indicating a higher m value. The observed structures and mode numbers are also confirmed by calculations using the above-mentioned sheet current perturbation model. Finally, the frequencies of the modes are commensurate with the $3/2$ originating from a faster rotating, more central, surface. In some cases the $2/1$ mode locks as the $3/2$ mode continues to rotate, indicating its existence on a surface further in.

The $2/1$ mode generally appears at the highest heating powers, and usually in H-mode plasmas. The typical onset threshold is in the range $\beta_p \sim 0.4$–0.6, suggesting strong bootstrap drives required to trigger the mode (as expected from the theory). A sawtooth event is also generally required for the $2/1$ mode to be triggered, indicating a metastable nature, as expected from the small island size stabilizing terms in Eq. (1). In some cases Thomson scattering profiles indicate a density and temperature flattening in the vicinity of the $q = 2$ surface, indicating the possible island structure. Once in L mode the $2/1$ mode usually locks, after which a disruption often occurs, either at or before the plasma current ramp down. When the $2/1$ mode appears in H mode, it only locks at or after the transition to L mode—this is possibly associated with the poorer momentum confinement in L mode. It is possible that these L mode transitions are in turn a result of the $2/1$ mode growing to substantial size, leading to a significant loss of confinement (as is typical at conventional aspect ratio).

Turning to the $3/2$ mode, this generally occurs somewhat more readily than the $2/1$, with modest beam powers ($\sim$800 kW) and β_p values $\sim$0.4. As for the $2/1$ NTM (and expected from theory), the mode has a threshold in β_p, and requires a sawtooth trigger. It does not always lock, and is not usually followed by a disruption. An interesting case is shown in Fig. 3. Here island size plotted is based on a cylindrical estimate from magnetic measurements, which agrees with more detailed field line tracing calculations (within $\sim$5%). After excitation by a sawtooth (in this case on transition to H mode), the mode amplitude is maintained (with some transients due to further sawteeth and ELMs). The neutral beam is switched off at 250 ms, and the resulting fall in β_p is followed by a fall in mode amplitude, with the mode decaying completely (to noise levels shown here, but also disappearing entirely in spectrograms) as the discharge falls below the critical β_p for NTM growth. The response of mode amplitude to changes in β_p suggests a bootstrap drive for the mode, while the

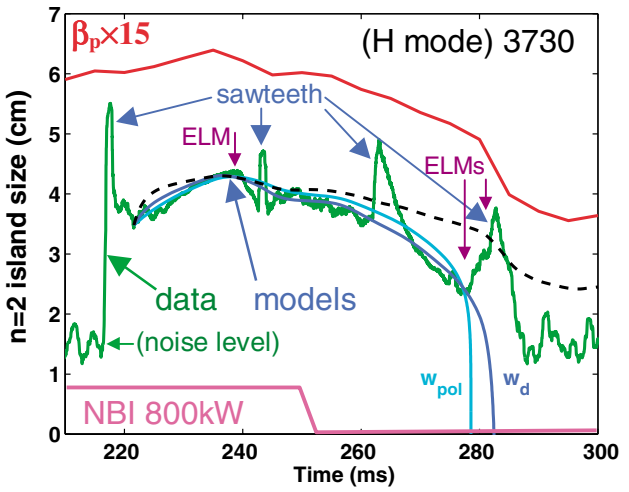

FIG. 3 (color). 3/2 mode amplitude evolution (green curve) in shot 3730, responding to β_p changes (red curve), after termination of beam heating (magenta curve). Also shown: results of modeling with ion polarization current (light blue curve), finite island transport (dark blue curve), or no (dashed curve) stabilization effects.

relatively large saturated island size from 220–260 ms indicates that Δ' must be negative to compensate for the bootstrap drive that will be present. The complete stabilization of the mode as β_p falls indicates the role of the $a_{\rm pol}$ or w_d stabilization terms in Eq. (1), which increase as island size shrinks. Modeling, necessary to confirm and explore these observations, is presented below.

An estimate of the effect of the 3/2 mode on confinement can be discerned from shot 2941 (Fig. 4). Here successive sawteeth (which excite small decaying $n = 2$ modes) briefly reduce the β_p value. However, when a high enough β_p is reached, a sawtooth excites a longer-lived 3/2 mode (with width ~6 cm). With the NTM, the β_p is observed to fall markedly further, and for longer, only recovering when the island size has decreased, after an L to H transition. Comparing thermal energy at 245 ms with pre-NTM trends (in these expanding plasmas), suggests a fall of ~3 kJ (11%) due to the NTM. This is comparable with estimates based on the Chang and Callen belt model [15], assuming pressure profile flattening over the island width, which predicts a fall of 2.4 kJ (consistent within uncertainties in q and pressure profiles in the reconstructions used). It is interesting to note that this mode is just marginally critical in β_p value, and starts to slowly decay shortly after seeding by the sawtooth. Subsequent regrowth of the mode may also be inhibited by changes to plasma profiles associated with the transition to H mode. Shot 2941 later experiences a much larger $n = 1$ mode at $\beta_p \sim 0.6$, after transition to H mode—ultimately followed by an H to L transition, locking, and disruption. As is typical, there are earlier excitations of this mode at lower β_p which decay away. Usually, only after higher performing H-mode plasmas are reached, are drives sufficient to sustain a 2/1 mode.

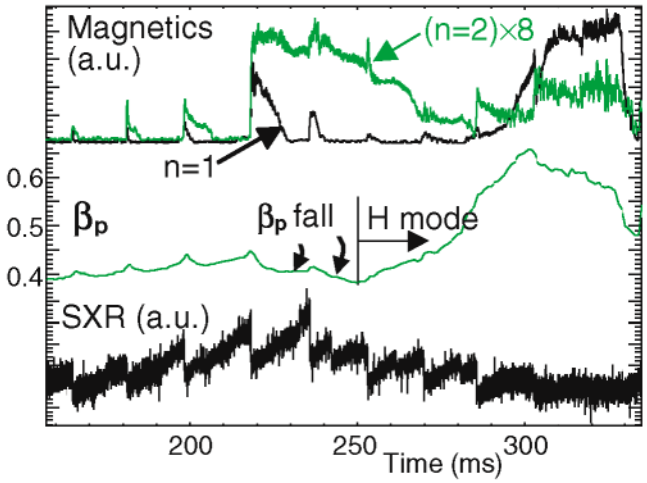

FIG. 4 (color). Impact of 3/2 mode on β_p in shot 2941; later a 2/1 mode is triggered at higher β_p following transition to H mode.

Generally, the 3/2 NTM is excited on MAST close to its saturated size, and at β_p values close to the critical β_p for mode growth. This contrast with conventional tokamaks, where the mode is usually triggered at higher β_p (well above the critical β_p), where the seed required is expected to be smaller (except when triggered at crashes after long sawtooth periods [16]). This indicates a strong seeding process in the ST, and might be expected due to the large inversion radius and strong toroidal coupling expected between modes in an ST.

To explore the underlying physics in more detail, we model discharge 3730 (shown in Fig. 3) using Eq. (1), but incorporating the correction of Ref. [12] for the form of the field curvature term. Theoretical predictions for coefficients are shown in Table I, calculated with forms valid at arbitrary aspect ratio and collisionality, using equilibrium reconstructions, and data including Thomson scattering and neutral particle analyzer measurements. For the bootstrap term, we take Ref. [17]: $a_{\rm bs} = 3.2\ (-L_{\rm bs})\ L_q/L_p$, where L_q and L_p are the q and pressure scale lengths (from equilibrium reconstructions and Thomson scattering profiles). Assuming similar electron and ion profiles, we can write $L_{\rm bs} = \eta_e/(1 + \eta_e)\ [L_{31}/\eta_e + R_{pe}(L_{31} + L_{32}) + (1 - R_{pe})(1 + \alpha)L_{31}]$, where $\eta_e = L_{ne}/L_{Te}$, $R_{pe} = p_e/p$, and the different terms represent

TABLE I. Comparison of theoretical and fitted parameters for island evolution in shot 3730.

Quantity	Theory	Fit: $w_d = 0$	Fit: $a_{\rm pol} = 0$
$r\Delta'$	−6.5	−6.5 (fixed)	−6.5 (fixed)
$a_{\rm bs}$	5.2	5.62	5.66
$a_{\rm GGJ}$	3.2	3.2 (fixed)	3.2 (fixed)
$a_{\rm pol}$(cm^2)	Uncertain	7.4	0 (fixed)
w_d (cm)	1.5–3.5[a]	0 (fixed)	1.45
τ_r (ms)	530[b]	100	100

[a]Dependent on transport model assumed.
[b]Usually reduced in conventional tokamak fits.

the density, electron temperature, and ion temperature contributions. In our case, $L_{31} \approx -0.72$, $L_{32} \approx 0.03$, and $\alpha \approx -0.37$, which gives $-L_{\rm bs} = 0.65$, assuming $\eta_e = 1$. The field curvature term is proportional to the resistive interchange term D_R [12], evaluated with the CHEASE code [18] using the experimental reconstructed equilibrium. The $a_{\rm pol}$ term is extremely uncertain, because of aspect ratio effects (large aspect ratio formulas were previously used [7]), and a strong dependence on mode rotation frequency in the frame where the radial electric field is zero (not yet measurable on MAST)—thus no predicted value is given. The w_d term is expected to be of the order of $\varepsilon^{1/2}\rho_\theta \approx 2.3$ cm, which is in the range of conductive or convective transport estimates given in Table I [10]. The value of $r_s\Delta'$ is estimated from the saturated island width and the theoretically predicted field curvature and bootstrap terms: $r_s\Delta' \approx -r_s\beta_p(a_{\rm bs} - a_{\rm GGJ})/w_{\rm sat} \approx -6.5$.

Fits to the observed island evolution are performed with different island stabilization models (w_d or $a_{\rm pol} = 0$, or $w_d = a_{\rm pol} = 0$). The key test is whether a good fit can be achieved with physically reasonable values for adjusted parameters. The fitting process takes the island size at some initial time point, and the time history of β_p, but no information about subsequent mode amplitude evolution. As the driving term is essentially proportional to $(a_{\rm bs} - a_{\rm GGJ})$, only one of these (we choose $a_{\rm bs}$) is varied. The results are shown in Fig. 3 and Table I. The agreement with measured island size evolution is remarkable, with either stabilization model allowing a close match to behavior (apart from sawtooth and ELM induced transients) until the mode disappears. With no stabilization model the fall in island size cannot be reproduced.

The agreement of fitted parameters with theoretical predictions (Table I) is particularly encouraging, especially given that such comparisons have previously been made only at conventional aspect ratios (over double that of MAST). There has been no need to change $r\Delta'$, and the bootstrap term is very close to theoretical expectations (validating the theoretical prediction for $a_{\rm bs} - a_{\rm GGJ}$). For the island transport model, the value of w_d is also comparable with theoretical estimates. A key difference is in the resistive time scale, which is substantially lower in order to allow the mode to evolve sufficiently quickly. This is often the case in conventional aspect ratio fits, indicating that the island itself may affect resistivity in its vicinity—this requires further investigation theoretically. The curvature term is about 60% of the bootstrap drive (compared to 10%–20% in conventional tokamaks). However, with flatter density profiles, the difference between bootstrap and field curvature terms would be reduced, which could be beneficial in H-mode plasmas (studies on ASDEX Upgrade [19] confirm that peaked density profiles lower NTM thresholds). Also, field curvature effects would be expected to dominate further with higher plasma current (so higher β/β_p) or lower shear.

To conclude, NTM physics has been tested in the new and significantly different regime of the ST, where the close agreement between fitted and theoretical parameters provides a remarkable validation of the theory. Behavior is similar to that at conventional aspect ratio, with low mode numbers (3/2 and 2/1), confinement degradation, a requirement for a seed perturbation and sufficiently high β_p. However, in these discharges the seed islands are more readily produced by the large sawteeth present, leading to modes close to the NTM (minimum) critical β_p. Modeling highlights the significance of field curvature effects, confirming previous theoretical arguments. This indicates that flatter density profiles, higher shaping, higher plasma current, or increased collisionality should increase stability to NTMs. The significance of threshold stabilizing terms is also confirmed—either ion polarization current or finite island transport effects can explain behavior. These results highlight the importance of optimizing plasma profiles in the ST. Future work should focus on development of off axis current drive techniques, and exploration of scenarios where field curvature effects are stronger. However, prospects remain positive due to the ST's naturally high shaping capability, which allows efficient operation with high edge and central safety factors, thus avoiding seeding instabilities or the NTM itself.

This work was jointly funded by the U.K. Department of Trade and Industry and EURATOM. O. S. is supported in part by the Swiss National Science Foundation.

*Permanent address: Centre de Recherches en Physique des Plasmas, Association EURATOM-Confédération Suisse, EPFL, 1015 Lausanne, Switzerland.

[1] J. A. Wesson and A. Sykes, Nucl. Fusion **25**, 85 (1985).
[2] F. Troyon *et al.,* Phys. Lett. A **110**, 29 (1985).
[3] A. Sykes *et al.,* Phys. Rev. Lett. **84**, 495 (2000).
[4] Z. Chang *et al.,* Phys. Rev. Lett. **74**, 4663 (1995).
[5] R. J. Buttery *et al.,* Plasma Phys. Controlled Fusion Suppl. B **42**, 61 (2000).
[6] R. Carrera, R. D. Hazeltine, and M. Kotschenreuther, Phys. Fluids **29**, 899 (1986).
[7] O. Sauter *et al.,* Phys. Plasmas **4**, 1654 (1997).
[8] M. Kotschenreuther, R. D. Hazeltine, and P. J. Morrison, Phys. Fluids **28**, 294 (1985).
[9] H. R. Wilson *et al.,* Phys. Plasmas **3**, 248 (1996).
[10] R. Fitzpatrick *et al.,* Phys. Plasmas **2**, 825 (1995).
[11] S. E. Kruger, C. C. Hegna, and J. D. Callen, Phys. Plasmas **5**, 455 (1998).
[12] H. Lutjens *et al.,* Phys. Plasmas **8**, 4267 (2001).
[13] J. W. Connor, F. L. Waelbroeck, and H. R. Wilson, Phys. Plasmas **8**, 2835 (2001).
[14] L. L. Lao *et al.,* Nucl. Fusion **25**, 1611 (1985).
[15] Z. Chang and J. D. Callen, Nucl. Fusion **34**, 1309 (1994).
[16] O. Sauter *et al.,* Phys. Rev. Lett. **88**, 105001 (2002).
[17] O. Sauter, C. Angioni, and Y. R. Lin-Liu, Phys. Plasmas **6**, 2834 (1999).
[18] H. Lutjens *et al.,* Comput. Phys. Commun. **97**, 219 (1996).
[19] J. Stober *et al.,* Plasma Phys. Controlled Fusion **43**, A39 (2001).